3-1-1995

Incorporation of Zn in GaAs during organometallic vapor phase epitaxy growth compared to equilibrium

W. Reichert
University of Utah, Salt Lake City, Utah

C.Y. Chen
University of Utah, Salt Lake City, Utah

W.M. Li
University of Utah, Salt Lake City, Utah

Jeffrey E. Shield
University of Nebraska - Lincoln, jshield@unl.edu

R.M. Cohen
University of Utah, Salt Lake City, Utah

See next page for additional authors

Incorporation of Zn in GaAs during organometallic vapor phase epitaxy growth compared to equilibrium

W. Reichert, C. Y. Chen, W. M. Li, J. E. Shield, and R. M. Cohen[a)]
Department of Materials Science and Engineering, University of Utah, Salt Lake City, Utah 84112

D. S. Simons and P. H. Chi
Chemical Science and Technology Laboratory, NIST, Gaithersburg, Maryland 20899

(Received 19 August 1994; accepted for publication 21 November 1994)

The zinc concentration measured after organometallic vapor phase epitaxy (OMVPE) growth on (100)-oriented GaAs at 700 °C has been compared to the zinc concentration measured after in-diffusion under near-equilibrium conditions. During diffusion, the concentration of Zn 20 nm below the surface was found to vary with $P_{Zn}^{1/2}$, as expected for bulk solid–vapor equilibrium. During growth, the concentration of Zn varied linearly with P_{Zn} up to a maximum value which was found to correspond to the solubility limit set by second phase formation, e.g., growth of Zn_3As_2. Although large differences were observed between the results of the two experiments when using nominally identical ambient conditions, all of the results are consistent with a thermodynamic model in which the Fermi level at the surface is pinned approximately 200 meV below the intrinsic Fermi level. Typical OMVPE growth conditions appear to give a bulk zinc concentration which is supersaturated relative to the ambient partial pressures used, and to enhance the diffusion of Zn into the substrate. © *1995 American Institute of Physics.*

I. INTRODUCTION

An improved understanding of the point defect mechanisms controlling diffusion in GaAs would help in designing process steps that minimize unwanted diffusion, particularly in heavily doped devices. Basic models of organometallic vapor phase epitaxy (OMVPE) growth[1] typically assume that when using a volatile dopant, the solid and vapor can be approximated as being in equilibrium. This implies that the point defect concentrations are close to their equilibrium values, and that any observed diffusion during growth is characteristic of equilibrium at the chosen ambient conditions. However, a number of growth results do not appear to follow simple thermodynamic predictions. In this article, we report the first experiments which demonstrate that the bulk Zn concentration and the characteristic diffusion lengths, found using typical OMVPE growth conditions, differ significantly from those found when solid–vapor equilibrium is closely approximated. The differences can be reconciled within a thermodynamic model which assumes that the Fermi level is pinned at the surface during processing.

A linear increase in dopant concentration with dopant partial pressure is commonly observed[2,3] up to a limiting concentration during OMVPE growth when using volatile dopants such as Zn in the vapor. Thermodynamic explanations[1] for this behavior have often ignored the fact that the dopant will become charged when it is incorporated into the solid. If the charge is included, equilibration between substitutional Zn in the solid and Zn in the vapor is summarized by the reaction

$$Zn_v + 1/4\,As_4 \leftrightarrow Zn^-As + p^+, \tag{1}$$

where the substitutional Zn concentration, $[Zn_{Ga}](\equiv N_{Zn})$, hole concentration, p, and partial pressures, P, are related (assuming activity coefficients of unity) via

$$K_1 = [Zn_{Ga}]p/P_{Zn}P_{As_4}^{1/4}, \tag{2}$$

which predicts $N_{Zn} \sim P_{Zn}^{1/2}$ when $p = N_{Zn}$ and when equilibrium between the vapor and bulk of the solid has been reached.

If, however, the Fermi level is pinned at the surface during diffusion, such that $p_{surface} < p_{bulk}$, then one expects from Eq. (2) that $N_{Zn,surf} \sim P_{Zn}$ and that $N_{Zn,surf} > N_{Zn,bulk}$. The equilibrium value, $N_{Zn,bulk}$, is expected to be *unaffected* by the space charge layer adjacent to the surface. If the Fermi level was pinned at an energy close to the intrinsic Fermi energy, then the thickness of the space charge layer could be estimated by assuming a simple depletion layer approximation. For example, if $N_{Zn} \approx 10^{19}$ cm^{-3} at $T = 700$ °C, then $x_d = [2\epsilon_s \Delta\phi/qN_{Zn}]^{1/2} \approx 8$ nm. In fact, the band bending extends over an additional 2–3 Debye lengths (L_D), and for these conditions we calculate $L_D \approx 2.3$ nm. Thus, when equilibrium is reached between Zn in the solid and the vapor under conditions such as these, one expects N_{Zn} to correspond to the bulk concentration beyond a depth of about 12–15 nm, and to be larger in the space charge region adjacent to the surface.

The importance of Fermi level pinning on the grown-in dopant concentration during liquid phase epitaxy (LPE) has been discussed previously.[4] During LPE, the liquid metal forms a Schottky junction with the GaAs, and several dopants incorporate in the solid with a linear dependence on the dopant activity in the liquid. Zn, however, has been found to have a solubility in GaAs which varies with the square root of its activity in the liquid at $T = 1000$ °C. This has been attributed to a combination of slow growth rate and high Zn diffusivity which allows equilibration to take place between

a)E-mail: richard.cohen@m.cc.utah.edu

 0021-8979/95/77(5)/1902/5/$6.00

the liquid and the bulk of the solid. To date, it appears that Fermi level pinning at the solid–vapor interface during OMVPE growth has not been established.

II. EXPERIMENTAL

GaAs epilayers of thicknesses 1–2 μm were grown by atmospheric pressure OMVPE on Si-doped GaAs substrates, (100)-oriented and cut 3° off toward (110), containing an electron concentration $n \approx 10^{18}$ cm^{-3}. Growth was performed in a rectangular OMVPE quartz reactor with a cross section of 2×5 cm. The sources used were TMGa (trimethylgallium), TBAs (tertiarybutylarsine), and DMZn (dimethylzinc), and the carrier gas was purified H_2. Electronic mass flow controllers were used to accurately control the partial pressures of all species, and the total flow rate used was 2.0 slm. An IR heat source was used to control the temperature of a graphite susceptor during growth. Temperature calibration was made by observing the melting of Sb and InSb. We have assumed that the ideal gas law applies for our calculations and that the organometallic sources have decomposed completely above the surface of the samples.

Undoped epilayers grown at T_g=650 °C, with an input V/III=56 and $P_{TBAs}=2.39\times10^{-3}$ atm, were found to be unintentionally doped with n~low-10^{15} cm^{-3} when using a nominal growth rate of 2 μm/h. The background doping in these epilayers is less than the intrinsic carrier concentration, n_i, at the growth temperature.[5] These undoped epilayers function as substrates for diffusion, i.e., substrates that contain reproducible point defect densities at the beginning of each diffusion experiment. Diffusion from the vapor into these undoped substrates was performed at T=700 °C, $P_{As_4}=6.0\times10^{-4}$ atm, and a total flow in the reactor of 180 sccm with different values of $2.27\times10^{-4} \leqslant P_{Zn} \leqslant 5.67\times10^{-3}$ atm. The resulting N_{Zn} near the surface was compared to N_{Zn} obtained after OMVPE growth under similar ambient conditions. An epilayer, with $N_{Zn}=8\times10^{18}$ cm^{-3}, was also grown for 2 h on top of an undoped substrate. The in-diffused Zn concentration profile obtained from this experiment was compared with the Zn concentration profiles obtained by in-diffusion from the vapor.

The solubility limit for Zn in GaAs is set by the formation of a second phase, i.e., Zn_3As_2. Growth of this second phase was obtained when the total gas flow through the reactor was reduced to 85 sccm and when using partial pressures of $P_{Zn}=1.20\times10^{-2}$ atm and $P_{As_4}=1.25\times10^{-3}$ atm. The solubility limit for Zn in GaAs was estimated by measuring N_{Zn} after in-diffusing Zn from the vapor using a P_{Zn} slightly less than that required for growth of Zn_3As_2.

Diffusion experiments were performed in the same quartz reactor as growth but the susceptor was replaced by a rectangular graphite oven, schematically shown in Fig. 1, that maintained a uniform temperature. The graphite oven fits snugly within the quartz reactor above the IR heater, and has a small hole (not shown) drilled in one end for a thermocouple. A 3×30 mm slit cut through the block holds the GaAs samples which lie face down on a single piece of GaAs acting as a proximity cap. With this diffusion system, no damage to the sample surface occurs even after several hours at elevated temperatures. The total gas flow rate is typically one order of magnitude below that used for growth. The low flow rate conserves sources during diffusion and also serves to crack the organometallic sources efficiently.

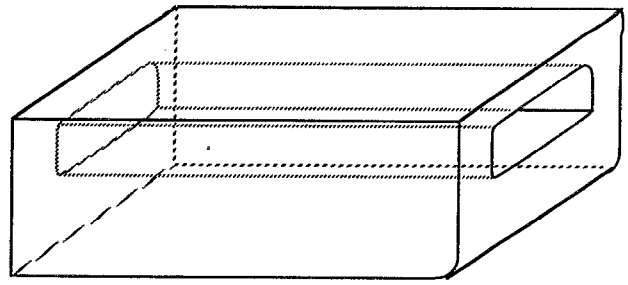

FIG. 1. Schematic diagram of the graphite oven used for diffusion studies. During diffusion, the oven is used in place of the growth susceptor in the OMVPE reactor, and the GaAs sample and proximity cap reside in the machined slit.

For either diffusion or growth, one should consider how many variables need to be controlled. Application of the Gibbs phase rule to a three component system (Ga, As, and Zn), in which there is a vapor phase and one condensed phase, gives three degrees of freedom. Thus, exactly three thermodynamic variables must be controlled to allow the vapor and the near-surface region of the solid to approach equilibrium. The variables we have controlled are T, P_{Zn}, and $P_{As,Total}$. Once these variables are set, the activity of all species, i.e., As_4, As_2, Ga, and vacancy and interstitial point defects, are thermodynamically determined at equilibrium. For the conditions we have used, we expect that $P_{As_4} = 1/4\ P_{As,Total}$ to a good approximation.

In performing diffusion in an open tube environment, another key question arises: after controlling the chosen three degrees of freedom, is it possible for the remaining uncontrolled partial pressures to approach their equilibrium values directly over the solid surface? For example, P_{Ga} above the surface is provided only by sublimation of the solid. One simple and practical way of keeping P_{Ga} close to its equilibrium value with a minimum of sublimation is to use a GaAs proximity cap. Because of the extremely low value of P_{Ga} over GaAs, $P_{Ga,eqm}$ can be attained through the sublimation of a small fraction of one monolayer. Our calculations show that the loss of Ga out of the dead space between the two pieces of GaAs into the reactor is very low, i.e., several hours are required at our annealing temperatures for even one monolayer to sublime. Adding volatile species to the reactor ambient such as Zn or As, with partial pressures 8–10 orders of magnitude higher than that of Ga, is effective because these species can quickly diffuse from the ambient into the space between the two pieces of GaAs. Thus, by choosing the appropriate thermodynamic variables to control during diffusion while using a proximity cap, equilibrium between the vapor and the near-surface region of the solid can be approached. Under these well-defined and controlled conditions, the concentration of all species, including point defects, are expected to approach their equilibrium values in the near-surface region of the solid. These concentrations then can be described in terms of the chosen degrees of freedom, as discussed elsewhere.[6,7]

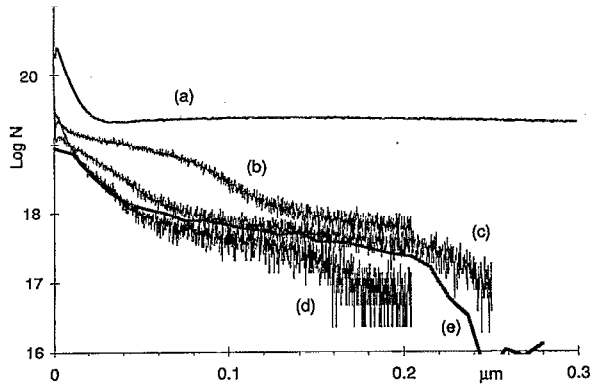

FIG. 2. Zn concentration (cm^{-3}) vs depth (μm) below surface after a 2 h diffusion with P_{Zn}=(a) 5.67×10^{-3} atm, (b) 1.70×10^{-3} atm, (c) 5.67×10^{-4} atm, and (d) 2.27×10^{-4} atm. Curve (e) shows the Zn concentration profile below a Zn-doped epilayer after a 2 h growth period.

Electrochemical capacitance voltage (C-V) profiling and secondary ion mass spectroscopy (SIMS) were used to measure the carrier concentration and the Zn concentration, respectively. High resolution SIMS depth profiles of Zn were made with a Cs^+ primary ion beam at an impact energy of 5.5 keV and an incidence angle of 42 degrees from normal, with detection of $ZnCs^+$ secondary ions. Using these SIMS measurement conditions with undoped GaAs, the sputtered ion signal for Zn (an artifact obtained near the surface) dropped 1 order of magnitude per ≈6 nm of etching. The concentration scale factor was determined by profiling a Zn ion implant of known dose in GaAs and correcting for isotopic abundance. Depth scale calibration was done by stylus profilometry of individual craters.

III. RESULTS AND DISCUSSION

For the diffusion of Zn from the vapor into undoped epilayers, the Zn concentration profiles taken by SIMS in the first 0.3 μm below the surface are shown in Fig. 2. The profiles correspond to values of P_{Zn} of (a) 5.67×10^{-3} atm, (b) 1.70×10^{-3} atm, (c) 5.67×10^{-4} atm, and (d) 2.27×10^{-4} atm. In all cases, there is a spike in N_{Zn} near the surface. With the etching conditions used, we believe that at least a portion of this spike represents a true increase in N_{Zn}, although the absolute accuracy of the concentration in this spike is uncertain. The surface spike can be related to at least two effects: the cooldown procedure used, and Fermi level pinning at the surface.

When the oven heater and the DMZn were simultaneously turned off at the end of a diffusion run, we observed significantly larger Zn spikes at the surface than those shown in Figs. 2(a)–2(d). Because of the low total flow rate used, P_{Zn} remained nearly constant upstream of the oven during the initial 2–3 min of cooldown. Since the solubility of Zn increases (for a fixed P_{As_4} and P_{Zn}) as the temperature decreases, the surface concentration can rise above the 700 °C value. In addition, a small amount of Zn_3As_2 may grow on the surface during cooldown. For the data shown in Figs. 2(a)–2(d), the DMZn was turned off 10 min prior to turning off the oven heater.

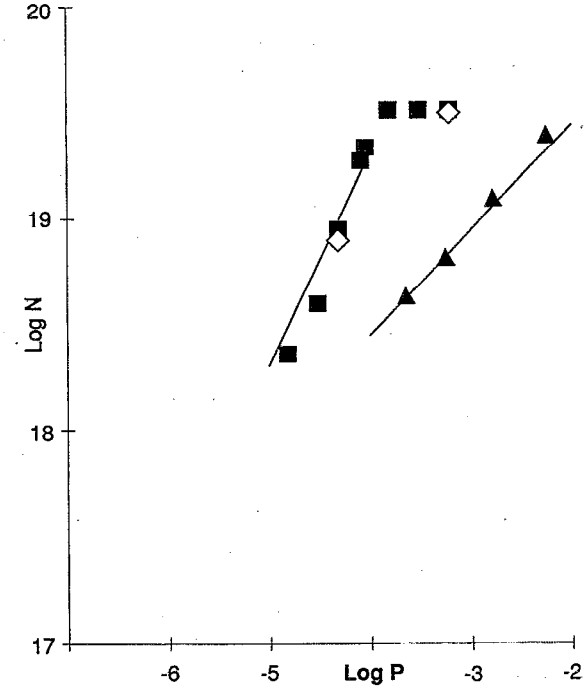

FIG. 3. Zn concentration (cm^{-3}) vs P_{Zn} (atm) for growth, as measured by CV (■) and SIMS (◇), and for diffusion (▲). The surface concentration, taken from the diffusion studies, follows the expected dependence on P_{Zn} when solid–vapor equilibrium can be approximated.

Figure 2(a), which we consider to be the most reliable of the profiles, indicates that the SIMS signal stabilizes at a depth of approximately 20 nm rather than at the 12–15 nm estimated above. The reason for this difference is unclear at present, and we shall assume that measurements representative of the bulk concentration are found at a depth of 20 nm. This approximation to the equilibrium concentration is summarized by the triangles in Fig. 3. The line shown through these data is drawn with a slope of 0.5, and the data closely fit the expected $N_{Zn,bulk}\sim P_{Zn}^{1/2}$.

We have also made a qualitative comparison between Zn diffusion into an undoped layer: (1) from the vapor and (2) from a growing epilayer, using similar ambient conditions and time. A Zn-doped GaAs epilayer, 1.3 μm thick, was grown for t=2 h on top of an undoped epilayer at T=700 °C with a constant $N_{Zn}=8\times10^{18}$ cm^{-3} in the epilayer. Significant Zn diffusion into the undoped layer was observed and Fig. 2(e) shows the Zn concentration profile beginning at the substrate–epilayer interface. The Zn profile is similar to that observed for in-diffusion from the vapor in Fig. 2(c), where the P_{Zn} used was more than an order of magnitude larger.

The interstitialcy (kick-out) mechanism is generally believed to govern the diffusion of Zn. For in-diffusion from the vapor, this implies that the Zn profile is controlled by the I_{Zn} concentration near the surface (where it quickly equilibrates with the P_{Zn} used). Conversely, if I_{Zn} in a growing epilayer is close to equilibrium with the vapor, then one expects the concentration of I_{Zn} at the doped–undoped interface to be no larger than its equilibrium concentration and the Zn profile in the (originally) undoped substrate to be no deeper than the profile observed after in-diffusion from the

vapor with the same P_{Zn}. Observation of the deeper profile, in Fig. 2(e), strongly suggests that I_{Zn} in the growing epilayer is supersaturated relative to the ambient vapor. These results have significant implications for the interpretation of interdiffusion data in semiconductors and we shall discuss those effects elsewhere.

During the OMVPE growth of Zn-doped epilayers, N_{Zn} increases approximately linearly with P_{Zn} at low partial pressures, and then stops increasing above about $P_{Zn} \approx 1\times10^{-4}$ atm, as summarized in Fig. 3 by the square data points and a line shown with unity slope. These data were taken by C-V measurements, and the two confirmed by SIMS are shown with diamonds in Fig. 3. These results are similar to those previously reported by Glew[2] and Okamoto *et al.*[3] for the OMVPE growth of Zn-doped GaAs using AsH_3. Similar to these reports, we have observed increased Zn incorporation as the growth temperature is lowered, but those results are not shown here. At lower P_{Zn}, the results are consistent with a Fermi energy which is pinned at the surface, i.e., a model of equilibrium which predicts $N_{Zn} \sim P_{Zn}$ at the surface. As growth proceeds, the surface continually becomes the bulk and $N_{Zn,epi} \sim P_{Zn}$ is thus observed after growth.

The results shown in Fig. 3 clearly show that N_{Zn} obtained from growth is much greater than the equilibrium value of N_{Zn} estimated after in-diffusion from the vapor, and that N_{Zn} in the grown epilayer is supersaturated relative to the ambient partial pressures. The supersaturated Zn concentration in the bulk of the epilayer must move toward its equilibrium value over time. The means for this to occur include precipitation and out-diffusion of Zn, i.e., substitutional Zn atoms move to interstitial sites and migrate to either the surface or the undoped substrate. We found no evidence from optical or transmission electron microscopy (TEM) of second phase formation during growth. As discussed above, the enhanced Zn diffusion into the substrate during growth appears to be related to an excess concentration of I_{Zn}.

If the Fermi energy at the surface were pinned exactly at the intrinsic Fermi energy, E_i, then the diffusion and growth curves of Fig. 3 would be expected to cross at $N_{Zn}=n_i \approx 2.5\times10^{16}$ cm^{-3}.[5] Although the intercept between the curves cannot be determined with a high degree of accuracy, it appears that they intercept near $N_{Zn}=3\times10^{17}$ cm^{-3}. From Eq. (2), the intercept of the two curves at low concentration corresponds to both solid–vapor equilibrium *and* flat bands in the GaAs, i.e., $N_{Zn,surf}=p_{surf}=N_{Zn,bulk}$. Thus, from the intercept, one may make an estimate of the Fermi energy at the surface,

$$E_i - E_f = kT \ln(p/n_i) \approx 200 \text{ meV}.$$

During subsequent diffusion experiments, we raised the source partial pressures further to learn the conditions required for second phase formation, i.e., to determine the solubility limit. A second phase was grown at $T=700$ °C using $P_{Zn}=1.2\times10^{-2}$ atm and $P_{As_4}=1.25\times10^{-3}$ atm and then characterized by TEM. Selected area diffraction (SAD) patterns revealed the second phase to be α-Zn_3As_2 (we have not tried to distinguish between the α and α' phases which have a slightly different lattice constant[8]). We found no evidence from SAD or x-ray diffraction for the formation of

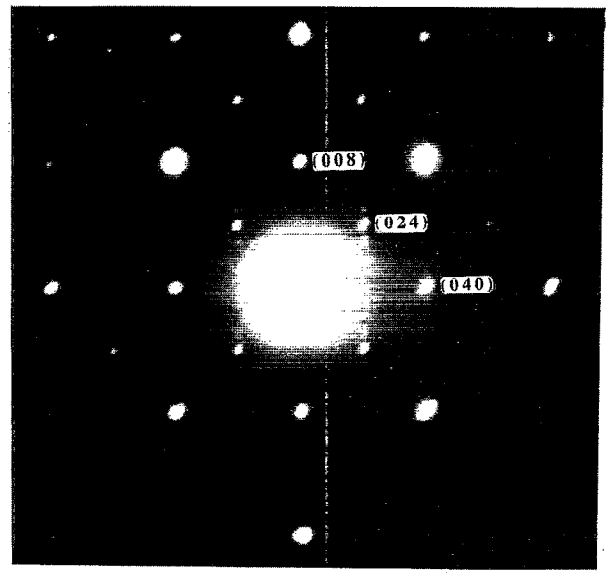

FIG. 4. Selected area diffraction pattern of the α-Zn_3As_2. The satellite spots near the (008), (040), and (024) reflections arise from the ordering of the vacancies on the Zn sublattice.

$ZnAs_2$, and this is consistent with thermodynamic data[9] which predict that $ZnAs_2$ will not form at the P_{As_4} we have used. Zn_3As_2 has an anti-fluorite structure in which 1/4 of the Zn sites are vacant. Above 651 °C, the β-phase (in which the vacancies are disordered) is stable.[10] As the temperature drops below 651 °C,[10] the vacancies readily order and a tetragonal unit cell defines the α'-phase where the lattice parameters for the α'- and β-phase are related by $a_{\alpha'}=2a_\beta \approx 11.8$ Å and $c_{\alpha'}=4a_\beta \approx 23.6$ Å.[8] For $T<190$ °C, a slight distortion of the structure occurs to give the α-phase. The ordering of vacancies along the c axis is evident in Fig. 4 as weak satellites adjacent to the (008), (024), and (040) reflections. It is interesting to note that epitaxial growth was also observed, i.e., $[001]_{Zn_3As_2} \| [001]_{GaAs}$, $[100]_{Zn_3As_2} \| [100]_{GaAs}$, etc.

We have attempted to determine the solubility limit, i.e., N_{Zn} in the GaAs after diffusion from a grown Zn_3As_2 layer on the surface, but we were unable to find an etchant which would remove Zn_3As_2 without simultaneously etching GaAs. Performing diffusion with a P_{Zn} slightly below that required to grow Zn_3As_2 yields very rapid diffusion and $N_{Zn}=2$–3×10^{19} cm^{-3} which is virtually the same as the maximum N_{Zn} obtained from OMVPE growth of GaAs at the same T and P_{As_4}.

Preliminary work at $T<700$ °C indicates that the N_{Zn} obtained in the plateau region of the N_{Zn}-P_{Zn} growth curve is also set by the solubility limit determined by second phase formation. Using lower growth temperatures, we have grown samples with $N_{Zn}=8\times10^{19}$ cm^{-3} and annealed them for 2 h at temperatures as high as 750 °C (where this N_{Zn} is supersaturated). N_{Zn} decreased by out-diffusion, but we found no evidence of precipitation with the TEM, in contrast to reports of Zn_3As_2 precipitation for comparable annealing times at 900 °C.[11] Since Zn_3As_2 contains a high density of vacancies, the formation of precipitates was presumably suppressed at

our temperatures by a low flux of vacancies from the GaAs surface.

The N_{Zn} observed just below the surface during the in-diffusion study can be compared to the results of Casey and Panish[12] who performed a closed ampoule equilibrium diffusion using a $ZnAs_2$-Zn_3As_2-GaAs source with average atomic composition 5/50/45 Ga/As/Zn. Our estimate for the bulk concentration, N_{Zn}, should be related to their N^*_{Zn}, taken near the surface, via[12]

$$N_{Zn}=N^*_{Zn}\left[\frac{(P_{Zn}/P^*_{Zn})(P_{As_4}/P^*_{As_4})^{1/4}}{\gamma_p/\gamma^*_p}\right]^{1/2}, \quad (3)$$

where γ_p is the activity coefficient of holes, and the quantities denoted by * are evaluated for the conditions used by Casey and Panish. Using an electron microprobe, they measured a surface concentration $N^*_{Zn}=2.4\times10^{20}$ cm^{-3} for $T_{diff}=700$ °C. From the work of Lyons,[9] they estimated $P^*_{As_4}\approx0.24$ atm in their ampoule. From the work of others at higher temperatures, they adjusted for Zn activity coefficient and estimated $P^*_{Zn}\approx7\times10^{-3}$ atm. From their $T=800$–1000 °C data, Casey and Panish estimated $\gamma_p\approx0.5$ when $N_{Zn}=2\times10^{20}$ cm^{-3} and $\gamma_p\approx1$ when $N_{Zn}\leqslant7\times10^{19}$ cm^{-3}. Using the above equation to extrapolate the Casey and Panish results to the diffusion conditions at our highest P_{Zn}, we would predict a surface concentration $N_{Zn}\approx7\times10^{19}$ cm^{-3}, which is about 2–3× higher than we have observed and in reasonable agreement with our results.

We have analyzed several possible reasons for this difference. The N_{Zn} measurements appear to be reasonably accurate, and there is no way to compare the P_{As} data of Lyons. Some limited estimates were gathered for γ_p at $T=700$ °C by Casey and Panish[13] which suggest that γ_p is sharply lower than the values used above. This would lower the predicted N_{Zn}, but it should be noted that they considered their high temperature estimates of γ_p to be more reliable. After examining Fig. 2(a), one might wonder if $N_{Zn}\sim10^{20}$ cm^{-3}, at a depth of ~10 nm, is indicative of the equilibrium concentration. If it were, then our diffusion coefficient, D_{Zn}, would need to be $\approx10^4$× smaller than the D_{Zn} observed by Casey and Panish in order to obtain the profile of Fig. 2(a). Adjustments to their D_{Zn} can be calculated,[7,12,14] but the effects of lower N_{Zn} and P_{As_4} approximately cancel out and little change in D_{Zn} is expected. Thus, N_{Zn} in the space charge layer cannot correspond to $N_{Zn,bulk}$ and there is no simple explanation for the discrepancy between the measured and predicted N_{Zn}.

IV. CONCLUSIONS

The zinc concentration resulting from OMVPE growth on (100)-oriented GaAs has been compared to the zinc concentration obtained from in-diffusion using similar ambient conditions. Large differences in N_{Zn} were observed under nominally similar conditions. However, both growth and diffusion are consistent with a thermodynamic model in which the Fermi level is pinned at the surface approximately 200 meV below the intrinsic Fermi level, i.e., the surface is in equilibrium with the vapor for both growth *and* diffusion. For diffusion, we conclude that

(a) $N_{Zn,bulk}$ can be estimated below the surface space charge region and follows the relation $N_{Zn}\sim P^{1/2}_{Zn}$, and
(b) $N_{Zn,surf}>N_{Zn,bulk}$ although $N_{Zn,surf}$ cannot be accurately determined because of measurement limitations.

For growth, we conclude that

(a) $N_{Zn,epilayer}\sim P_{Zn}$ because Fermi level pinning at the surface leads to $N_{Zn,surf}\sim P_{Zn}$ and $N_{Zn,surf}$ becomes the epilayer concentration as growth proceeds,
(b) $N_{Zn,epilayer}$ remains supersaturated relative to the vapor because D_{Zn} is not large enough, and the growth rate is not small enough, to allow equilibration between the bulk and vapor in a typical growth run, and
(c) the maximum N_{Zn} obtained from growth is the solubility limit determined by the formation of the second phase, Zn_3As_2.

We have observed enhanced Zn diffusion out of growing epilayers into undoped substrates, and this is consistent with a supersaturated N_{Zn} and I_{Zn} in the growing epilayer. These results suggest that an improved understanding of the Fermi pinning mechanism at the surface may lead to control over point defect concentrations, and thus over diffusion, during growth or post-growth annealing.

ACKNOWLEDGMENTS

Support from NSF through contract number DMR-9024848 is gratefully acknowledged.

[1] G. B. Stringfellow, J. Cryst. Growth **75**, 91 (1986).
[2] R. W. Glew, J. Cryst. Growth **68**, 44 (1984).
[3] K. Okamoto, H. Mawatari, K. Yamaguchi, and A. Noguchi, J. Cryst. Growth **98**, 630 (1989).
[4] H. C. Casey, Jr. and M. B. Panish, J. Cryst. Growth **13/14**, 818 (1972).
[5] J. S. Blakemore, J. Appl. Phys. **53**, 520 (1982).
[6] R. M. Cohen, J. Appl. Phys. **67**, 7268 (1990).
[7] R. M. Cohen, J. Appl. Phys. **73**, 4903 (1993).
[8] *Landolt-Bornstein Handbook, New Series*, edited by O. Madelung (Springer, New York, 1983), Group III, Vol. 17e.
[9] V. J. Lyons, J. Phys. Chem. **63**, 1142 (1959).
[10] *Binary Alloy Phase Diagrams, 2nd ed.*, edited by T. B. Massalski (ASM International, Materials Park, 1990), Vol. 1.
[11] W. Jager, A. Rucki, K. Urban, H. G. Hettwer, N. A. Stolwijk, H. Mehrer, and T. Y. Tan, J. Appl. Phys. **74**, 4409 (1993).
[12] H. C. Casey, Jr. and M. B. Panish, Trans. AIME **242**, 406 (1968).
[13] H. C. Casey, M. B. Panish, and L. L. Chang, Phys. Rev. **162**, 660 (1967).
[14] T. Y. Tan and U. Gosele, Mater. Sci. Eng. B **1**, 47 (1988).